Supplementary Figure Legends.

Supplementary Figure 1. Symmetry of the motor components and 3.9-nm thick serial sections. a) To detect the symmetry of the components in the average, annular masks were generated for the five different motor regions shown in the panel and then applied separately to all twenty individual particles. The regions that were not analyzed for symmetry are grey and transparent. The ruler on the left marks the heights of the radial sections shown in panels **c** and **d**. **b**) Rotational correlation coefficients were calculated by rotating each of the 100 objects (5 regions of 20 different motors) in 1° steps 360° around the z-axis and calculating the 3-D cross-correlation coefficient with the unrotated object. The results were Fourier transformed in 1-D to produce rotational power spectra (one for each component of each motor), and then the average power spectrum for each component was plotted, as shown in the panel. The only symmetry detected was the 16-fold symmetry within the stator ring, so this symmetry was imposed on the entire motor, effectively smoothing the other components. **c)** Sections through the average motor. (Section 9 is through the membrane.) **d)** Sections through the symmetrized average. Note the symmetry of the stators both below (sections 10-11) and above (sections 6-8) the membrane (scale bar 20 nm, for panels **b** and **c**).

Supplementary Figure 2. Significance maps. a) An axial cutaway of the symmetrized average map contoured at various levels. Because the connections are not all coplanar, the left and right halves of the figure actually show different planes. The left half shows the plane that bisects connection #4 (see Fig. 2 of main paper for numbering), while the right half bisects connection #1. The density threshold at which surface renderings of electron cryotomography maps should be contoured is usually unclear. The isosurfaces in Fig. 2 of the main paper correspond to 0.95 standard deviations above the mean. This value was chosen as the tightest contour that still manifests the connection between the

stator assembly and the C ring known to exist from previous work[1]. Here four additional contours are shown as well. The colors red, yellow, green, blue and pink correspond to 0.45, 0.75, 0.95, 1.2 and 1.45 times the standard deviation, respectively. The steepest density gradients exist along the edges of the rod, while the most gradual occur at the edge of the stator assembly where the membranes of the individual motors continue outwards with somewhat variable curvature. The order of the connections in terms of density are, from largest to smallest, #2, #1 and #4, and finally #3. **b)** A 2 nm-thick, axial section of the symmetrized variance map with the outline of the motor superimposed (at the favored, 0.95 standard deviation contour level, colored again in green). The highest variances occur around the rod, as expected since the rods in each individual motor emerge at different angles, bending over against the P-collar and underneath the outer membrane. The next highest variances are in the cytoplasm underneath the rotor. Some variance is seen in the regions of the connections, as well as on the top face of the export bundle. The rotor and stator stud regions of the map have the least variance. **c)** An axial cutaway of a symmetrized significance map, generated by subtracting from the normally-distributed average map the product of 2.093 times the standard error map, which corresponds to the lower boundary of the "95% confidence" interval of a two-tailed student t-test for a sample size of 20[22]. The colors red, yellow, green, blue and pink correspond to thresholds of 0.31, 0.41, 0.51, 0.61 and 0.71 times this map's standard deviation, respectively. The middle threshold (0.51, green) was chosen to again enclose the same favored volume as the isosurface in Fig. 2 of the main text. While the absolute numerical confidence level is not known because the "correct" threshold is still somewhat arbitrary, the order of the connections, in terms of significance from greatest to least, is #4, #1, #2, and finally #3, which alone lacks some connecting density at the favored threshold.

Supplementary figures 3-5 show sequence alignments for the three key motor proteins FliG, MotA, and MotB, which argue that their domain structure is conserved throughout bacteria. Though *Treponema primitia* strain ZAS-2 has not been sequenced, its 16S rRNA shares 86% and 85% sequence identity with that of *T. pallidum* and *T. denticola*, respectively. Thus the structural inferences about the positions, sizes, and interactions of their domains made here based on our *T. primitia* reconstruction are likely generally applicable. The organisms compared are the Gammaproteobacteria *E. coli* and *Salmonella typhimurium*, the Betaproteobacteria *Bordetella bronchiseptica*, the Spirochetes *Treponema denticola*, *Treponema pallidum*, *Leptospira interrogans* and *Borrelia burgdorferi*, the Firmicute *Bacillus subtilis*, *Thermotoga maritima*, the Epsilonproteobacteria *Helicobacter pylori*, the Deltaproteobacteria *Geobacter sulfurreducens* and the Alphaproteobacteria *Agrobacterium tumefaciens*, except that in Fig. 3, *Agrobacterium tumefaciens* has been replaced with *Caulobacter crescentus*. Amino acids with 50% conservation are shaded in gray while those with 100% identity are shaded in black. The sequences were aligned with ClustalW[23] and presented using Alscript[24].

Supplementary Figure 3. Sequence alignment of FliG. The colored alpha-helices below the sequences are from the crystal structure of *T. maritima's* middle and C-terminal domains of FliG[19]. The pink region corresponds to the middle domain; the blue region corresponds to the 2-nm long helix that bridges the middle and C-terminal domains and the orange and green regions correspond to the C-terminal domain. Amino acids shaded in cyan are those which, when mutated in *E. coli*, caused reduced binding to FliM in yeast 2-hybrid studies[25]. Notice they occur in both domains. The blue-colored and red-colored arrowheads are the conserved positively- or negatively-charged amino acids that interact with the oppositely-charged residues of MotA.[1]

Supplementary Figure 4. Sequence Alignment of MotA. The colored helices correspond to the predicted transmembrane helices (TMH) generated by the TMHMM Server[26]. The blue helices correspond to the predicted helices of *T. pallidum*; the orange helices to *T. maritima*'s and the green helices to *Salmonella*'s. The blue-colored and red-colored arrowheads are the conserved positively- or negatively-charged amino acids that interact with the oppositely-charged residues of FliG.[1]

Supplementary Figure 5. Sequence Alignment of MotB. The colored helices are predicted and colored as in Figure 2. The pink arrowhead points to the conserved, protonatable aspartate residue.[1] The black line bounded by arrowheads delineates the OmpA-like domain that binds to the peptidoglycan layer. Also aligned are the chain sequences from the crystal structures of the *E. coli* Peptidoglycan-associated lipoprotein (PDB id: 1OAP) and the OmpA-like domain from *N. meningitidis* RmpM (PDB id: 1R1M).

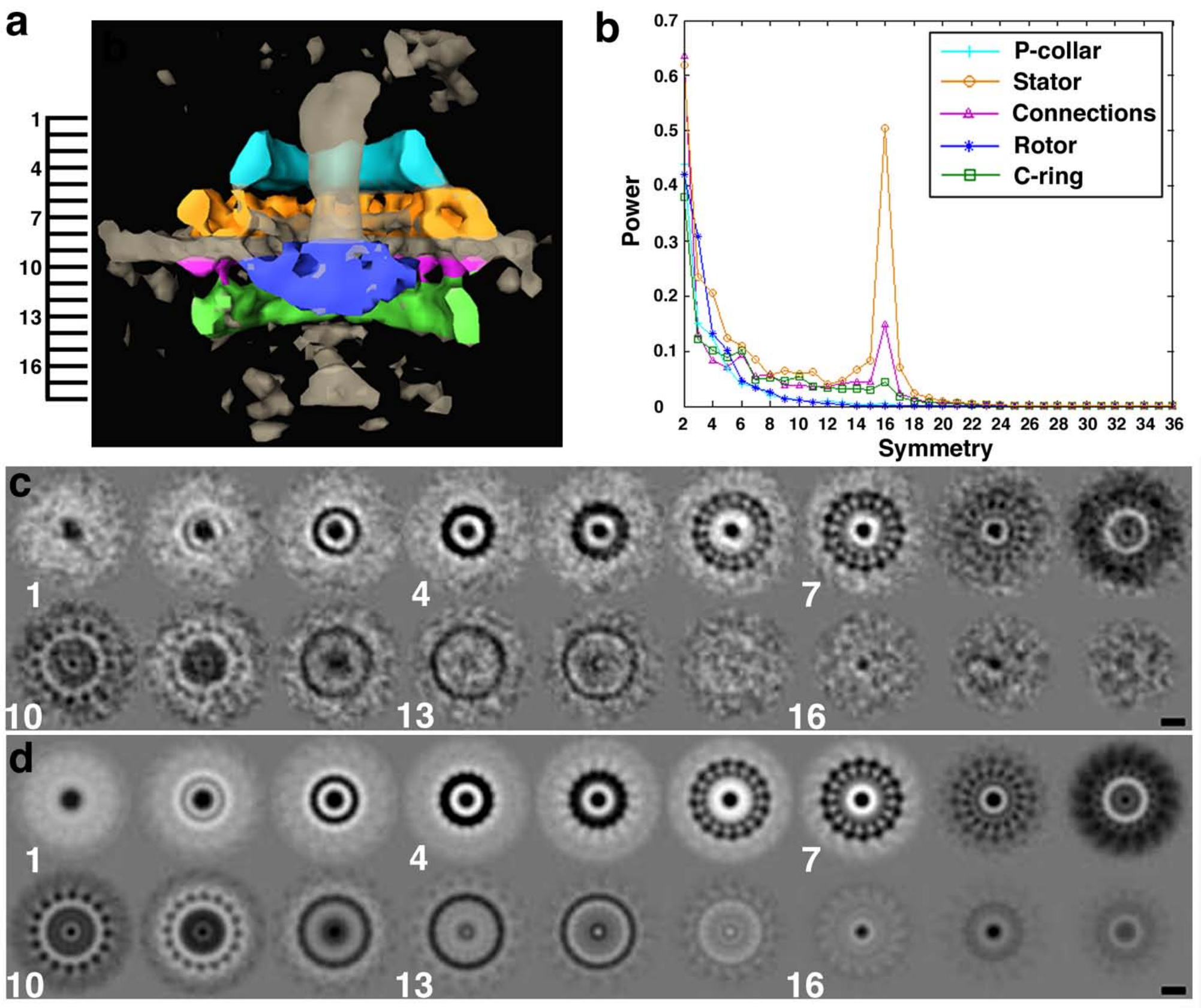
a
1
4
7
10
13
16
b
Power
Symmetry
P-collar
Stator
Connections
Rotor
C-ring
0
0.1
0.2
0.3
0.4
0.5
0.6
0.7
2 4 6 8 10 12 14 16 18 20 22 24 26 28 30 32 34 36
c
1
4
7
10
13
16
d
1
4
7
10
13
16

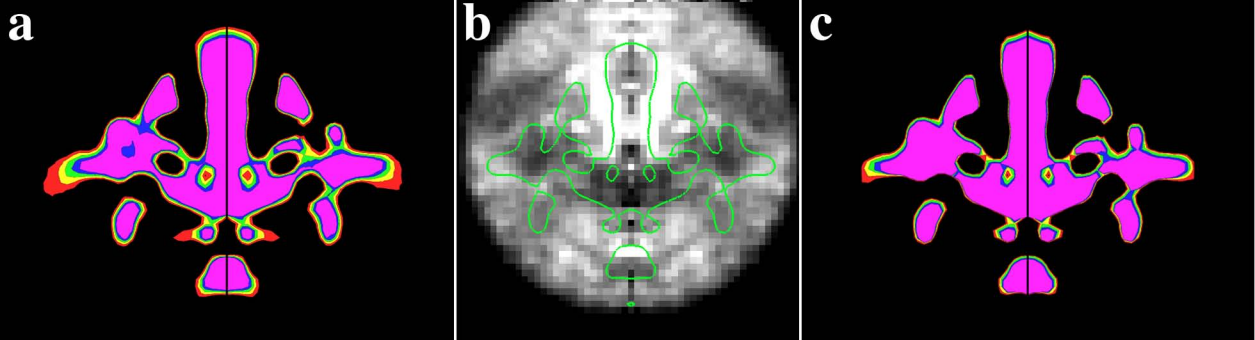
a
b
c

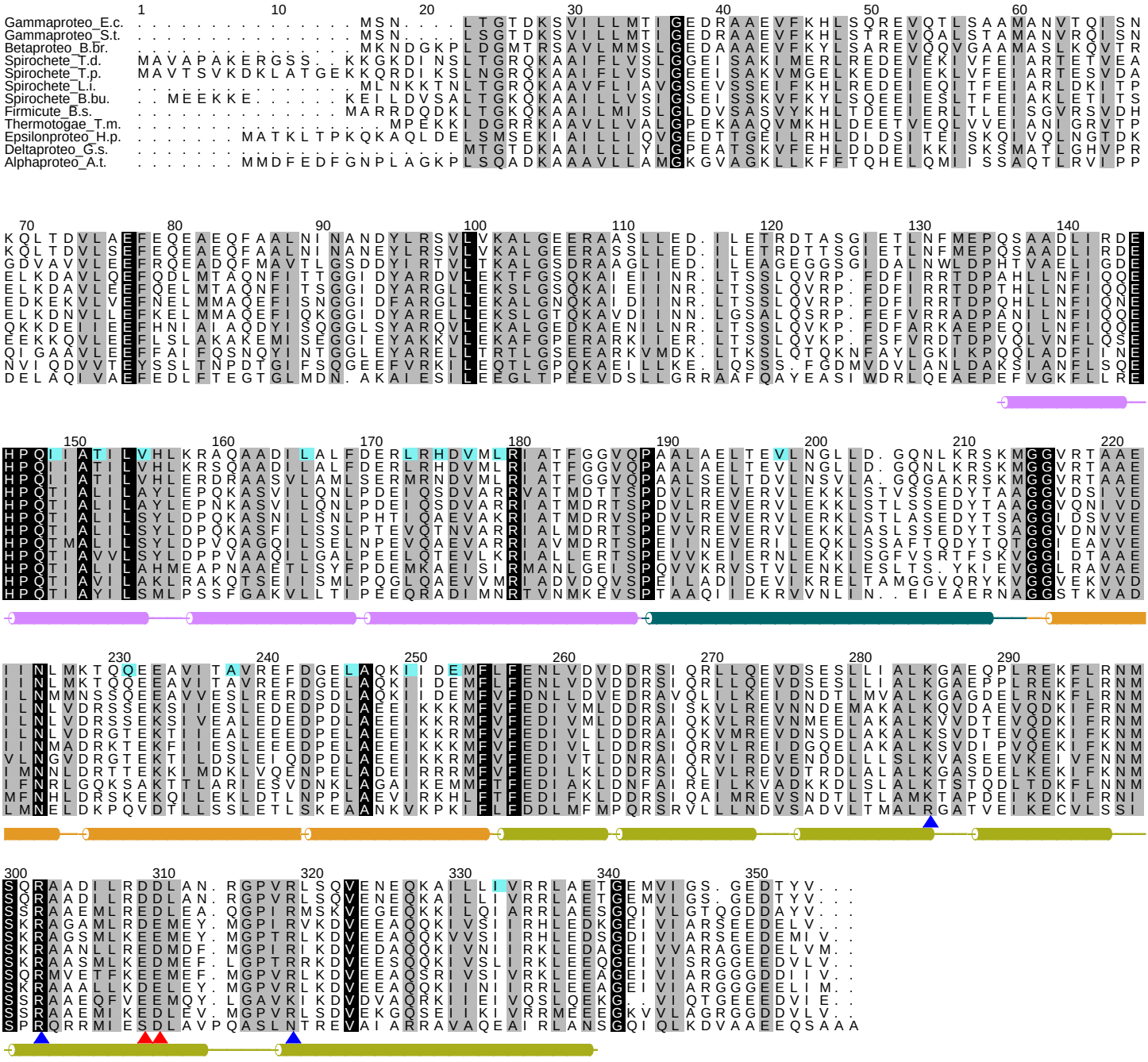
Gammaproteo_E.c.
Gammaproteo_S.t.
Betaproteo_B.br.
Spirochete_T.d.
Spirochete_T.p.
Spirochete_L.i.
Spirochete_B.bu.
Firmicute_B.s.
Thermotogae_T.m.
Epsilonproteo_H.p.
Deltaproteo_G.s.
Alphaproteo_A.t.

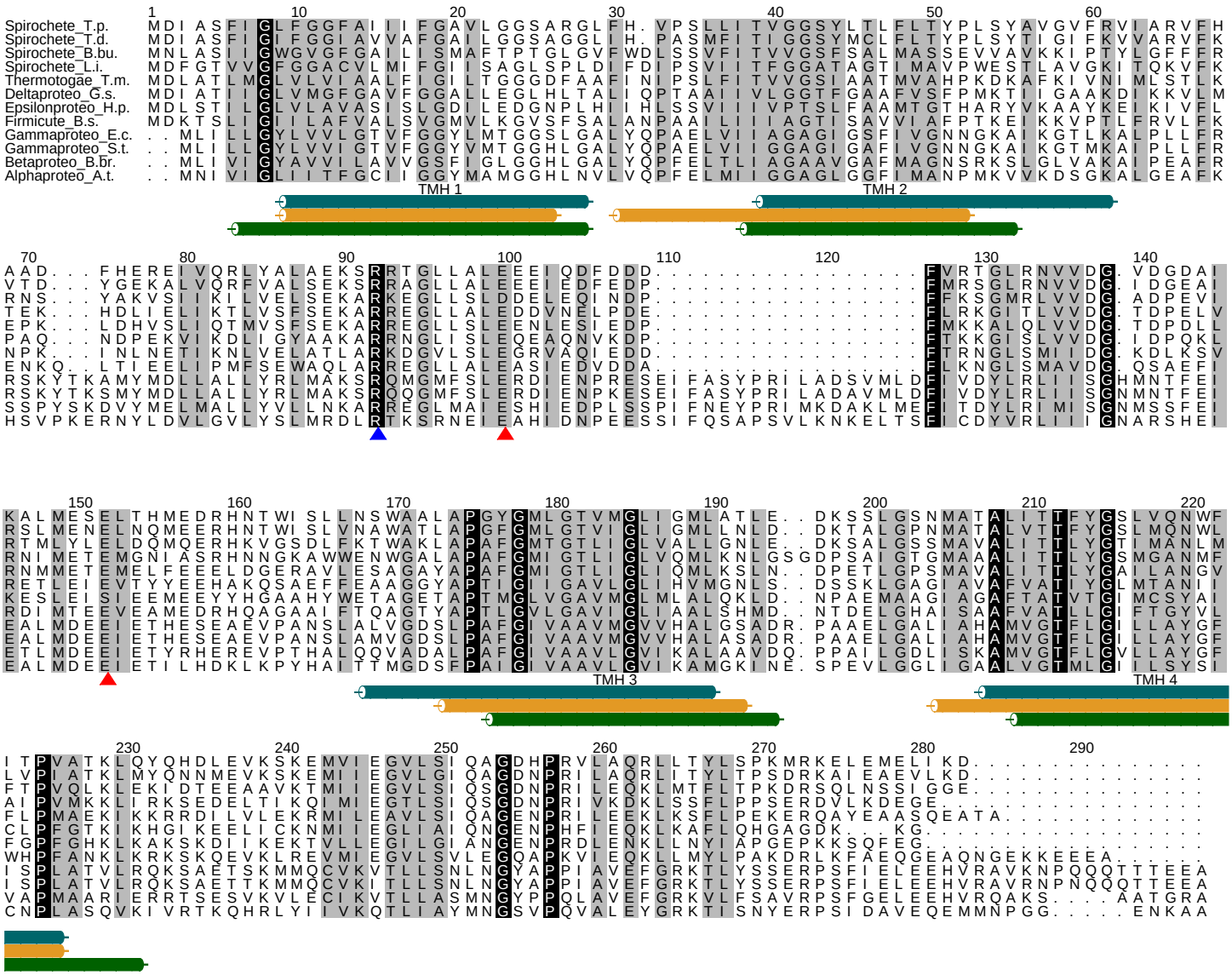
Spirochete_T.p.
Spirochete_T.d.
Spirochete_B.bu.
Spirochete_L.i.
Thermotogae_T.m.
Deltaproteo_G.s.
Epsilonproteo_H.p.
Firmicute_B.s.
Gammaproteo_E.c.
Gammaproteo_S.t.
Betaproteo_B.br.
Alphaproteo_A.t.
TMH 1
TMH 2
TMH 3
TMH 4

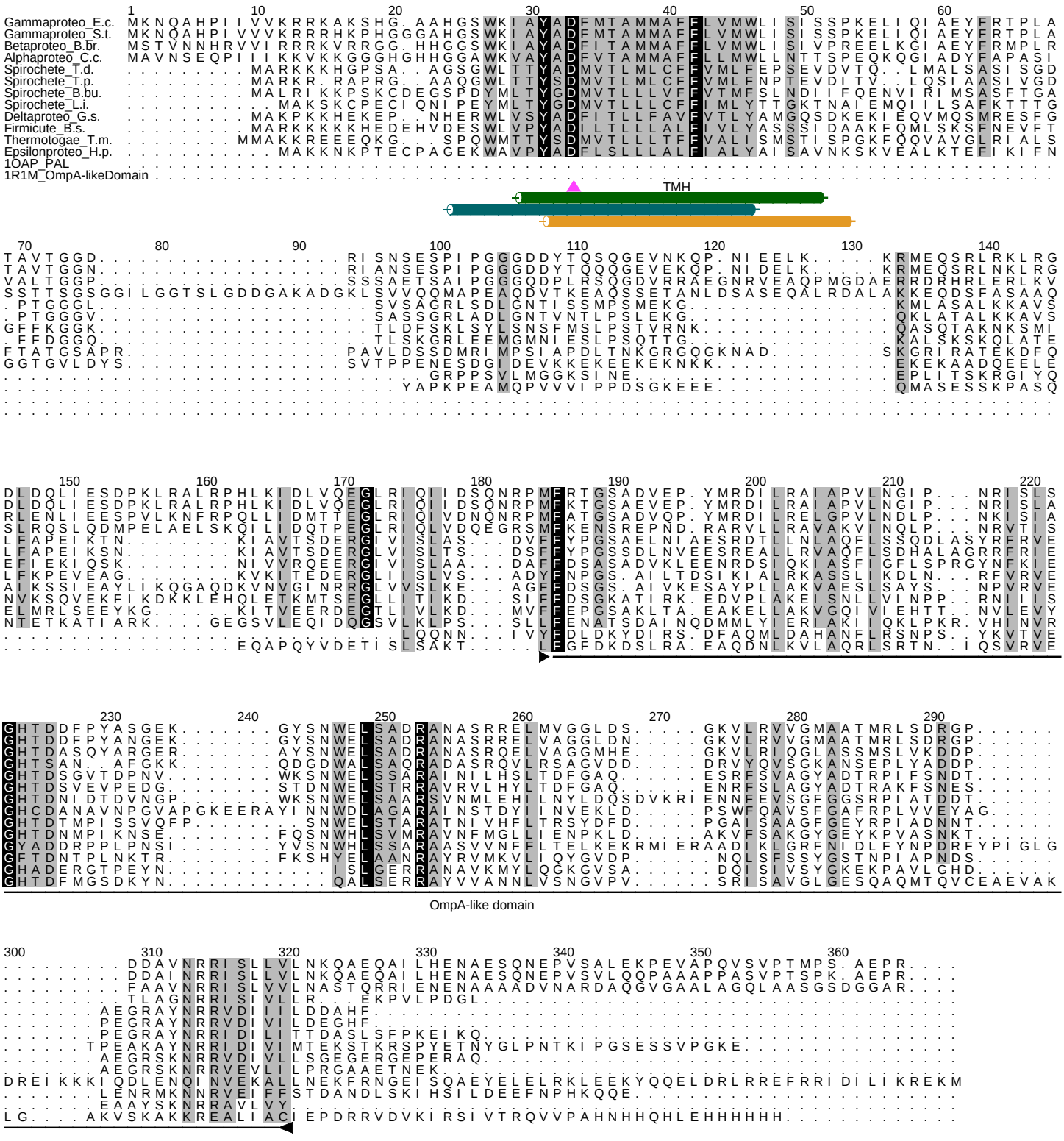
Gammaproteo_E.c.
Gammaproteo_S.t.
Betaproteo_B.br.
Alphaproteo_C.c.
Spirochete_T.d.
Spirochete_T.p.
Spirochete_B.bu.
Spirochete_L.i.
Deltaproteo_G.s.
Firmicute_B.s.
Thermotogae_T.m.
Epsilonproteo_H.p.
1OAP_PAL
1R1M_OmpA-likeDomain
TMH
OmpA-like domain

Supplementary Movie

The movie first shows orthoslices from top to bottom through the reconstruction of one *T. primitia* cell and then displays the segmented surfaces of tip filaments (green), the outer membrane (brown), the inner membrane (pink), the two periplasmic flagella (blue and red), and the surfaces of the motors for each flagella (blue and orange). An isosurface of the averaged, symmetrized flagellar motor is shown next (yellow), and finally the components that are thought to spin are colored in blue while the fixed stator region is shown in yellow and orange.

Supplementary Methods

Cell Growth and Grid Preparation. Cultures were grown to an OD of ~0.6 at room temperature in sealed culture tubes containing 4YACo medium under a headspace of 80% H_2 and 20% CO_2 as described previously[21]. To prevent aggregation in high-salt solutions, 10-nm colloidal gold was pretreated with 5% BSA for 30 minutes. It was then concentrated five-fold and 5 ml was applied to glow-discharged, carbon-coated R 2/2 quantifoil grids and then dried. Grids were plunge frozen in a Vitrobot (FEI Company) in 100% humidity.

Electron Tomography Data Collection and 3-D Reconstruction. Tilt series were acquired using the UCSF Tomo software[27]. Typically, tilts were incremented 1º from –63º to 63º. The magnification was 22,500 (0.98 nm/pixel) and the total dose was ~110 $e^-/Å^2$, distributed according to the 1/cos scheme. Tomograms were reconstructed using IMOD[28].

Image Processing. Bsoft[29] and the Peach distributed computing system[30] were used for image processing. Visualization and surface map measurements were done with Amira

(Mercury Computing Systems). The twenty extracted particles were bandpass-filtered between 200 nm and the first CTF zero. The missing wedge in reciprocal space was masked so that only measured regions of reciprocal space were used to align the particles, but no other object-specific mask was used. Course alignments were done in refine mode with an initial angular step size of 5° through all three Euler angles. Map averaging, symmetrization, and significance testing were done as described in the main text and supplementary figure legends.

Supplementary Notes

22. Frank, J. Three-Dimensional Electron Microscopy of Macromolecular Assemblies (Academic Press, San Diego, 1996).

23. Thompson, J. D., Higgins, D. G. & Gibson, T. J. CLUSTAL W: improving the sensitivity of progressive multiple sequence alignment through sequence weighting, position-specific gap penalties and weight matrix choice. *Nucleic Acids Res*. **22**, 4673-80 (1994).

24. Barton, G. J. ALSCRIPT: a tool to format multiple sequence alignments. *Protein Eng*. **6**, 37-40 (1993).

25. Marykwas, D. L. & Berg, H. C. A mutational analysis of the interaction between FliG and FliM, two components of the flagellar motor of *Escherichia coli*. *J. Bacteriol.* **178**, 1289-94 (1996).

26. Krogh, A., Larsson, B., von Heijne, G. & Sonnhammer, E. L. Predicting transmembrane protein topology with a hidden Markov model: application to complete genomes. *J. Mol. Biol.* **305**, 567-80 (2001).

27. Zheng, Q. S., Braunfeld, M. B., Sedat, J. W. & Agard, D. A. An improved strategy for automated electron microscopic tomography. *J. Struct. Biol.* **147**, 91-101 (2004).

28. Kremer, J. R., Mastronarde, D. N. & McIntosh, J. R. Computer visualization of three-dimensional image data using IMOD. *J. Struct. Biol.* **116**, 71-6 (1996).

29. Heymann, J. B. Bsoft: image and molecular processing in electron microscopy. *J. Struct. Biol.* **133**, 156-69 (2001).

30. Leong, P. A., Heymann, J. B. & Jensen, G. J. Peach: a simple Perl-based system for distributed computation and its application to cryo-EM data processing. *Structure* **13**, 505-11 (2005).